OsloMet – Storbyuniversitetet
Fakultet for teknologi, kunst og design
Institutt for maskin, elektronikk og kjemi

TILGJENGELIGHET
Åpen

BACHELOROPPGAVE

BACHELOROPPGAVENS TITTEL	DATO
Exosomal yRNA in different stages of preclinical Alzheimer's disease	26.05.23
	ANTALL SIDER / BILAG 56
FORFATTERE Fanny Bendigtsen Schirmer Jenny Strand Eriksen	INTERN VEILEDER Tone Berge

UTFØRT I SAMARBEID MED	EKSTERN VEILEDER
Oslo universitetssykehus, Rikshospitalet Avdeling for mikrobiologi	Ingrun Alseth Ingrid Lovise Augestad

SAMMENDRAG
Alzheimer's disease (AD) causes a significant decline in cognition and the pathology is characterized by the accumulation of the peptides amyloid-beta and tau. The content of blood-derived exosomes are viewed as a potential biomarker for AD, and a good candidate may be yRNA.

The overall objective of this project is to investigate pathological mechanisms underlying AD. The 5XFAD transgenic mouse model, which has five human mutations associated with AD, will be used to collect plasma and organs and to do behavioral analyzes. Exosomes will be isolated from plasma samples and brain tissue.

Nanoparticle tracking analysis and Western blot was performed and the results indicated that there were exosomes in the samples for both wild type and 5XFAD mice, which was confirmed with transmission emission microscopy. Further, AD affected the size of plasma exosomes. Expression of brain yRNA was analyzed with reverse transcriptase quantitative polymerase chain reaction and the results show that AD affects the expression of *Rny3* in the brain in early compared to later stages of AD. The fluctuation of yRNA expression during AD progression should be further tested for the potential to be used as an indicator of disease severity.

Alzheimer's disease
Exosomes
yRNA

Table of Contents

OSLOMET

Summary

Alzheimer's disease (AD) causes a significant decline in cognition for the affected individual and the pathology is characterized by the accumulation of the peptides amyloid-beta (Aβ) and tau. Today, AD is diagnosed mainly by clinical assessment in addition to imaging. Promising candidates for early non-invasive diagnosis of AD are the use of blood biomarkers. The content of blood-derived exosomes are viewed as a potential biomarker. yRNA, which is a non-coding small RNA, is one type of molecule that can be found within exosomes. Higher amounts of yRNA have been found in exosomes compared to intracellular levels, which might indicate that yRNA and yRNA-derived fragments are good candidates as biomarkers for AD.

The aim of this project is to investigate pathological mechanisms behind AD. Levels of yRNA in exosomes and brain tissue isolated from mice will be analyzed to see if it can be used as a biomarker for AD. Wild type (WT) and 5XFAD transgenic mice will be used to collect plasma and organs at different ages. Behavioral analysis will be performed on the mice, in addition to immunofluorescence microscopy to look at inflammation and accumulation of Aβ plaque in the brain. Exosomes will be isolated from plasma samples and brain tissue, and then validated with nanoparticle tracking analysis (NTA), western blot and transmission electron microscopy (TEM). Expression of yRNA will be analyzed with reverse transcriptase quantitative polymerase chain reaction (RT-qPCR).

NTA showed that there are many particles in the plasma exosome samples, while TEM analysis confirmed the presence of exosomes for both WT and 5XFAD mice. Further, AD affected the size of plasma exosomes at an early stage of disease, but AD did not affect the number of secreted plasma exosomes. Immunofluorescence microscopy showed the presence and increase of Aβ plaques and inflammation in the brains of 5XFAD mice but not in WT. Finally, AD affects the expression of *Rny3* in the brain in early stages compared to later stages of AD. Even though there is a long way left to find a biomarker, our results indicate that AD affects both plasma exosomes and yRNA levels in brain tissue. This suggests that yRNA within exosomes is an interesting biomarker candidate in AD.

Abbreviations

AD	Alzheimer’s disease
APP	Amyloid precursor protein
Aβ	Amyloid-beta
cDNA	Complementary DNA
CNS	Central nervous system
C_T	Cycle threshold
dH_20	Distilled water
EV	Extracellular vesicles
EZM	Elevated zero maze
FAD	Familial alzheimer's disease
GAPDH	Glyceraldehyde 3-phosphate dehydrogenase
gDNA	Genomic DNA
IF	Immunofluorescence
MVB	Multi vesicular bodies
ncRNA	non-coding RNA
NTA	Nanoparticle tracking analysis
PET	Positron emission tomography
RT-qPCR	Reverse transcription quantitative polymerase chain reaction
SD	Standard deviation
SEC	Size exclusion chromatography
SLE	Systemic lupus erythematosus
TEM	Transmission electron microscopy
UC	Ultra-centrifugation
RIPA	Radioimmunoprecipitation assay buffer
RT	Reverse transcriptase
yRNA	Cytoplasmic RNA
WB	Western blot
WT	Wild type

1. Introduction

1.1 Dementia and Alzheimer's disease (AD)

Dementia is a disease that causes a significant decline in cognition that interferes with daily life, functioning, and behavior of those affected (1). As the leading cause of disability, about 47 million people lived with dementia in 2015, and by 2050 the number is expected to increase to 132 million (2). The underlying cause of dementia is brain atrophy due to neurodegeneration and the most common types of dementia are AD, vascular dementia, dementia with Lewy bodies and frontotemporal dementia. Dementia can also arise as a secondary injury to e.g. traumatic brain injury or ischemic stroke, or as a cause of Parkinson's disease (1). More than 50% with dementia have AD, which causes anxiety and loss of memory and cognitive abilities (3).

The pathology of AD is characterized by amyloid-beta (Aβ) and neurofibrillary tangles in the brain, in addition to inflammation. Amyloid plaques are the extracellular accumulation of misfolded Aβ, which is a peptide formed when amyloid precursor protein (APP) is cleaved. Neurofibrillary tangles are intracellular structures that are formed when the hyperphosphorylated protein, tau, accumulates (4). Amyloid plaques and neurofibrillary tangles cause blockage of cell communication, which will lead to loss of cognitive function when spreading (5). The accumulation of these misfolded proteins can start almost 20 years ahead of clinical symptoms. Therefore, researchers believe that the accumulation of pathologic proteins can be prevented by early interventions and diagnostics (6). Amyloid plaques, neurofibrillary tangles, and loss of neurons in brain tissue have been discovered in aged people not diagnosed with AD. Whether this means that they are normally aging, or if the discoveries are precursors to neurodegeneration is still unsure. Diagnosis is therefore not based on brain pathology, but on clinical tests (7).

AD is usually divided into two main types: 1) familial AD (FAD), also referred to as early onset, and 2) sporadic AD, referred to as late onset. Around 1% of all AD cases are FAD (5). FAD is caused by mutations in the genes for APP, presenilin 1 and presenilin 2. The mutations increase the production of Aβ (8). Sporadic AD is not associated with any genetic mutations.

However, some genes are suspected to increase the risk of developing AD such as the ε4 allele of apolipoprotein E (*APOE*). There are three alleles of *APOE*, and the ε4 is the second most common (~14%) (5).

In addition to genetic-related risks, other factors can increase the risk of AD such as a low education level, unhealthy diet, and lack of physical activity (3). There are no treatments that can reverse or stop the neurodegenerative process, but there are factors that can reduce the risk of AD (7). Some of these factors include physical activity, cognitive stimulation, and a low-calorie and low-cholesterol diet (3). Drugs used for the treatment of AD is targeting the underlying cognitive dysfunction and behavioral symptoms short-term, but does not reverse the neuronal damage (5).

Until recently AD could only be diagnosed through post-mortem analysis of brain tissue to confirm the presence of Aβ and tau proteins (9). Today, AD is diagnosed mainly by clinical assessment in addition to computerized tomography (CT) or magnetic resonance imaging (MRI) and blood tests to exclude other conditions (4). Lumbar puncture and positron emission tomography (PET) imaging have also been used, but the high invasiveness and costs regarding these methods have caused concern, which has been a catalyst for researchers to find new and less invasive ways of diagnosing AD. A promising candidate for early non-invasive diagnosis of AD is the use of blood biomarkers (10).

1.2 Biomarkers for AD

A biomarker can be defined as a biological molecule that indicate the presence of disease or other processes and can be found in bodily fluids, such as blood, cerebrospinal fluid, and urine, or tissues (11). Playing a major part in the processes of screening, diagnosing, monitoring, and treating diseases makes biomarkers a valuable resource in medicine (12). An ideal biomarker is highly specific, easily detectable, non-invasive, cost-effective, and reproducible (10). Having a highly specific biomarker can be described as a strong association between the biomarker and the condition; meaning that the marker should measure or predict clinical outcomes. Responding relatively to the condition is also important; the biomarker should fluctuate in response to treatment, or disease progression (12).

The search for a reliable and specific biomarker for AD is like looking for a needle in the haystack due to the variability in disease onset and progression from patient to patient (9). Heterogeneity of the pathology, and complexity of AD causes diagnostic difficulties, especially concerning late-onset AD (13). Being a disease with so many unknown sides and undiscovered pathophysiological processes to it, finding a single marker specific enough might not be possible. Multiple markers that reflect different aspects of AD are potentially needed (14).

Existing methods, like lumbar puncture and PET, can confirm the presence of current AD biomarkers, like Aβ-plaques and phosphorylated tau (15, 16). However, finding blood-based biomarkers for AD can establish less invasive and more cost-effective methods for diagnosing AD. The initial goal of AD research on biomarkers was to isolate a single plasma protein, *e.g.* Aβ, and that the analyte would correlate to the progression and pathology of AD (9). The complex composition of plasma makes the analysis of blood-based biomarkers challenging, and the continued search for a blood-based biomarker is an important field of research (9). In addition, the heterogeneity of the pathology of AD calls for the addition of new biomarkers to bring light to other aspects of AD (13).

1.3 Exosomes

In recent years the role of extracellular vesicles (EVs), especially exosomes, in AD has gained a lot of attention, both as a potential biomarker and as an option for treatment (17). EVs are secreted by most cells and contain biological molecules such as nucleic acids, proteins, and lipids, enclosed in a lipid bilayer (figure 1) (18). Different types of RNA have been found inside EVs, including messenger RNA, long non-coding (nc)RNA, circular RNA, and small ncRNA (19). These biomolecules can act as signaling molecules in recipient cells. EVs have surface molecules to make sure they deliver the information to the correct cells. By receptor-ligand interaction, endocytosis or phagocytoses, they deliver their content to the cytoplasm of the recipient cell. Some of the molecules that EVs transfer between cells are micro RNAs and other ncRNAs (18).

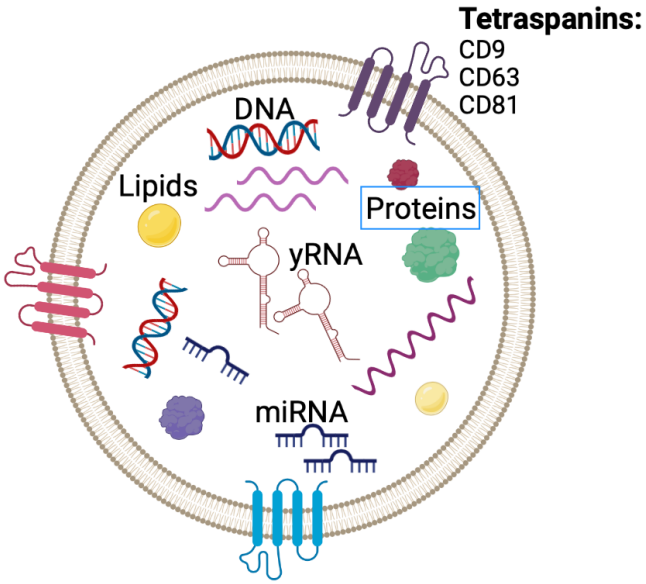

Fig. 1. Illustation of an exosome. Exosomes contain DNA, different types of RNA, lipids and proteins. The tetraspanins shown (CD9, CD63 and CD81) are transmembrane proteins found in all exosomes. Figure made in Biorender.

EVs are categorized by their size and how they are formed in the cell (20). Exosomes are a subtype of EVs, with an endosomal origin, and are created by double invagination of the plasma membrane until intracellular multivesicular bodies (MVB) are formed. The MVBs contain vesicles that are secreted as exosomes. EVs can range in size from 30 to 1000 nm in diameter, and exosomes have a diameter of about 40 to 160 nm (20).

Researcher are trying to find a standardized method for isolation and validation of exosomes and The International Society of Extracellular Vesicles (ISEV) have created a guideline for research on EVs and exosomes (21). For isolation, ultra-centrifugation (UC) has been the leading method. UC-methods give low recovery and purity, use large volumes, and are often time consuming. Alternative methods have been developed, and one of these methods is size exclusion chromatography (SEC), which is a size based separation method. Advantages of SEC includes rapid isolation of exosomes and usage of small sample volumes (22). Transmission electron microscopy (TEM) and nanoparticle tracking analysis (NTA) are two of the methods used for validation. Western blot (WB) is also used to validate exosomes based on membrane proteins i.e. tetraspanins like CD9, CD63 and CD81. These proteins can be found in the membrane of all exosomes, and is therefore commonly used as markers for exosomes (21).

The exact function of exosomes are not yet known, but they are likely involved in removing cell constituents and in intercellular communication (20). The environment and the type of cell where the exosome is created, can affect the content, and this is why the proteome of the exosome will reflect the originating cell proteome. Since the cell surface receptors on the exosomes can vary, the function of the exosomes also varies and can create different biological responses in the recipient cell (20).

Studies show that exosomes may have a role in the degradation of misfolded proteins (15). Both tau and Aβ are found in exosomes derived from cells in the central nervous system (CNS), and it is therefore likely that exosomes can spread these proteins as they are taken up by recipient cells (20). This means that exosomes may be central to the progression of neurodegenerative diseases like AD (15). CNS-derived exosomes can cross the blood-brain barrier and therefore have the potential to be used as a blood biomarker for neurodegenerative diseases (15). One of the most important biological molecules inside blood-derived exosomes, are ncRNAs (23, 24).

1.4 yRNA

Cytoplasmic (y)RNAs are a subgroup of small ncRNA of ~100 nucleotides. They were first discovered in Sjögrens disease and systemic lupus erythematosus (SLE) as components of ribonucleoproteins forming complexes with the autoantigens Ro60 and La proteins (25). The human genome codes for four different types of yRNAs; *RNY1, RNY3, RNY4*, and *RNY5*, while the rodent genome only encodes for two types of yRNA; *Rny1* and *Rny3* (19). Structurally, yRNAs consists of 4 different domains: loop domain, upper stem domain, lower stem domain and polyuridine tail, shown in figure 2. The loop domain both contain binding sites for proteins, as well as cleavage sites for yRNA fragmentation. All yRNAs have a long stem, containing the upper and lower stem domains. While the upper stem domain is central for replication, the lower stem domain contains the binding site for the autoantigen Ro60. Binding site for another protein closely linked to yRNAs, called La, can be found on the polyuridine tail (26). Between individual yRNA molecules, the primary and secondary structures differ slightly. In the nucleus, RNA-polymerase III is responsible for the transcription of yRNA. The binding of yRNA to the protein complex Ro60 enhances the export of yRNA out of the nucleus, into the

cytoplasm of the cell. In the cytoplasm, Ro60 is a factor in stabilizing yRNA, preventing degradation (19). It has been found that autoantigens Ro60 are targeted by autoantibodies in diseases such as Sjögrens and SLE, but whether the Ro60 complex actually contribute to pathogenesis has not been determined (27).

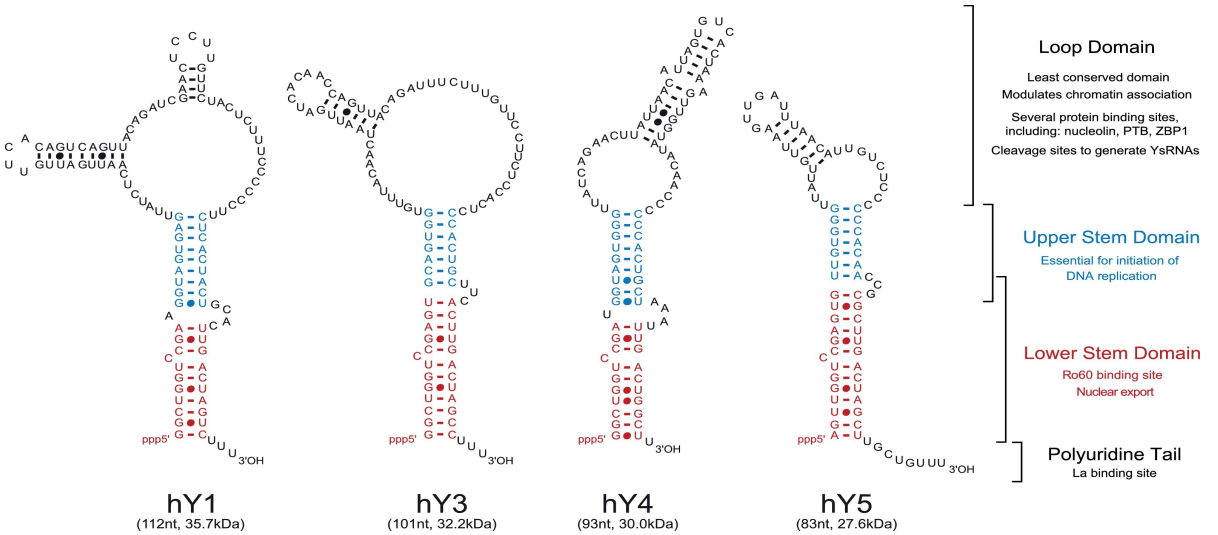

Fig. 2. The structure of the four non-coding yRNAs in the human genome. Size is given in kDa, and length is given in nucleotides (nt) for each yRNA. The loop domain, upper stem domain, lower stem domain and polyuridine tail are shown (26).

EV-RNA consists mostly of small ncRNA like yRNA, micro RNA, transfer RNA, and small nucleolar RNA (19). Exogenous stimuli on the donor cell can alter the composition of RNAs and change the molecular messages of EVs. The EV-recipient cells can undergo modifications and change in function as a response to components of EV. Further, the transfer of RNA through EVs between cells is a common and adaptable process of communication which is highly efficient (19).

When being transferred to a target cell through secretion in EVs, yRNA is believed to have signalling functions (19). The role of individual yRNAs as signal molecules and their effect on the target cell has not been determined. EVs meditate simultaneous transfer of other components such as lipids, proteins, and other types of RNA. Extracellular mediated yRNAs found in vesicles like EVs, and their function, is a recent subject of research. The number of studies uncovering their function is limited, but has shown immune-regulatory effects of yRNA, both pro- and anti-inflammatory (19).

A cells response to different types of stress such as disease, is associated with fragmentation of yRNA, where full-length yRNA is divided into smaller pieces (28). The fragments are categorized into short fragments of about 22-25 nucleotides, and longer fragments of about 31 nucleotides. Processes like apoptosis, aging and pathological mechanisms can increase the fragmentation of yRNA (25). The function of yRNA-derived fragments is still not entirely understood, but so far *RNY5* derived fragments originating extracellularly from human cancer cells have been shown to trigger rapid cell death in primary cells (29).

Levels of yRNA and yRNA-derived fragments in e.g., serum or urine from patients with diseases like breast cancer and leukaemia have been found to be higher compared to the yRNA levels in healthy patients (19). Further, many tumour cells have been found to release high amounts of EVs, which might be correlated to finding increased levels of yRNA and yRNA fragments (19). Finally, yRNA has been found in much higher amounts in exosomes compared to intracellular levels and this suggests that there is a selective packaging of yRNA into exosomes (30). This suggests that yRNA and yRNA-derived fragments are good candidates as biomarkers.

1.5 Preclinical models of AD

Studying AD in humans is challenging due to the heterogeneity of the disease and the limited amount of available human brain tissue to use for analysis (8). Therefore, it is necessary to use model systems with complexity close to the human brain. Although *in vitro* stem cell cultures are commonly used to model AD and other neurodegenerative diseases, transgenic mouse lines are most frequently used. However, mice do not develop dementia spontaneously so different human genes associated with the disease have been inserted into the genome of the mice to create various AD models. None of the current models include all aspects of AD pathology, i.e. both Aβ and tau, and most of them only include the accumulation of Aβ (31). The 5XFAD transgenic mouse line is a common preclinical model where two mutated human genes, *APP* and *PSEN1,* have been introduced in C57/BL6 mice. There are three mutations in the introduced human *APP* gene; Swedish (K670N/M671L), Florida (I716V) and London (V717I) and two mutations in the human *PSEN1* gene (M146L and L286V). The expression of these mutated

genes increase the Aβ production, which rapidly accumulates and causes amyloid plaque pathology in the mice. Already at 1,5 months, the amyloid plaque is starting to form in the brain and the cognitive decline has already begun at 4-5 months (8).

Behavioral tests are used to assess development and progression of cognitive decline in mice with AD pathology (32). AD leads to both memory deficits and anxiety-like behavior in mice. The Y-Maze and Morris water maze (MWM) assess spatial working memory and spatial learning. The MWM induces more stress in the animals, therefore the Y-Maze may be more suitable (33). Commonly used tests for unconditioned anxiety in mice is the elevated zero maze (EZM) and open field test (34) where the animals are allowed to freely explore the maze. More anxious animals tend to stay longer in the enclosed sections of the maze or close to the walls to avoid going into open spaces.

1.6 Objectives and aims

The overall objective of this project is to investigate pathological mechanisms underlying AD. Further, the main aim is to analyze levels of yRNA in exosomes and brain tissue isolated from mice with and without AD to see if there is a yRNA profile that can be used as a biomarker for AD.

To investigate this the 5XFAD transgenic mouse model will be used to collect blood plasma and brains at different time points during the progression of AD. Anxiety levels of all mice will be tested with the EZM and immunohistochemistry will be used to check for accumulation of Aβ-plaque. In addition, we will look at inflammation with Iba1, which is a microglia marker. Exosomes will be isolated from blood plasma from mice and identification and characterization of exosomes will be performed with WB, NTA and TEM. Finally, the expression of yRNA will be analyzed with reverse transcription quantitative polymerase chain reaction (RT-qPCR).

2. Materials and methods

All chemicals/solutions are listed in the appendix A.3.

2.1 Contributions

All methods including genotyping, isolation of exosomes, isolation of RNA from exosomes and brain tissue, TapeStation, NanoDrop, Qubit, WB and RT-qPCR were performed by Jenny S. Eriksen and Fanny B. Schirmer. Supervisor Ingrid Lovise Augestad performed behavior test of mice, blood plasma collection and organ harvesting, biopsies for genotyping, immunofluorescence (IF) and NTA. TEM images were taken by Espen Stang at Oslo Universitetssykehus (OUS).

2.2 Animal model and experimental design

Animal care and experimental procedures were in compliance with the Norwegian National Animal Research Authority and performed in accordance with the European Directive 2010/63/EU.

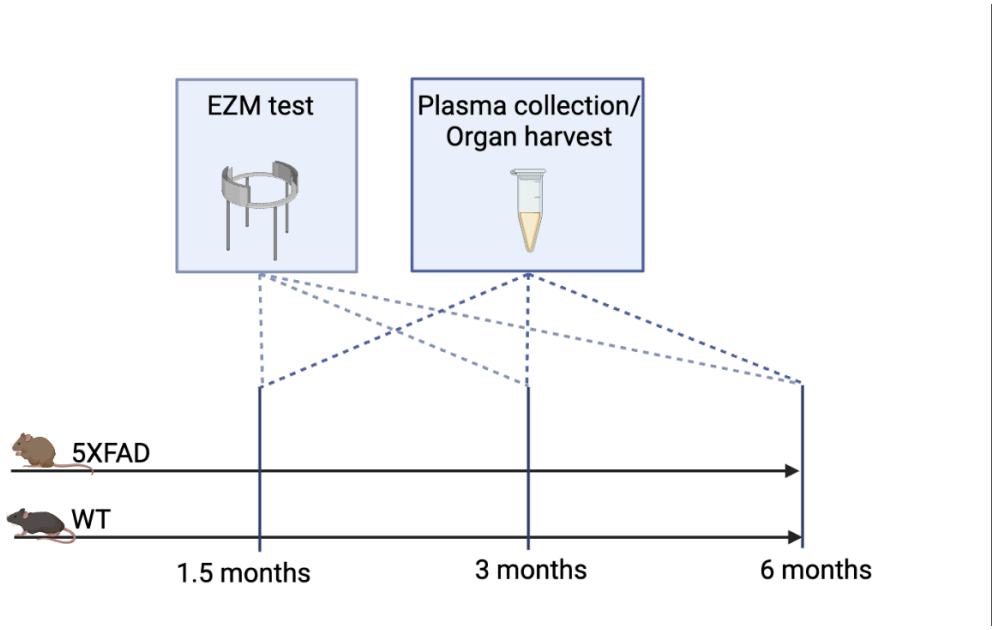

Fig. 3. Experimental design. EZM, plasma collection and organ harvest was performed for mouse at three ages, 1.5, 3 and 6 months (Biorender.com).

5XFAD mice (C57BL/6SJL;#034840-JAX, The Jackson Laboratory/Mutant Mouse Resources & Research Centers (MMRRC), USA) and wild type (WT) mice (C57BL/6J from Janvier, France and C57BL/6N from Taconic, USA) were used in this project.

Behavioral tests with EZM, explained in section 3.4, as well as plasma collection/organ harvest were performed on mice at 1.5 months (WT n = 9, 5XFAD n = 4), 3 months (WT n = 4, 5XFAD n = 4), and 6 months (WT n = 6, 5XFAD n = 4).

2.3 Genotyping

5XFAD mice are always bred with WT mice to create heterozygous animals, otherwise the phenotype will be too strong, *i.e* the mice will develop AD already from birth. Therefore, we need to genotype all mice to confirm if they carry the 5XFAD mutations or not. Ear and tail biopsies were used for genotyping as follows: 100 µL hot shot buffer was added to the tissue samples and the tubes incubated at 95°C for 20 min. 100 µL of neutralizing buffer was added to the samples to stop the reaction. A PCR master mix was made with primers specific for the 5XFAD genetic mutations (see appendix A.4). In a new PCR tube, 11 µL master mix and 1 µL of DNA from each sample being genotyped were added. The PCR reactions were run with the following PCR program on a thermo cycler (VWR Doppio):

1. 95°C for 3 min
   A. 95°C for 30 sec
   B. 60°C for 30 sec
   C. 72°C for 1 min
   D. 35 cycles A-C
2. 72°C for 5 min
3. Hold at 8°C

Biometra Power Pack P25 T and Hoefer HE33 Mini Horizontal submarine unit was used for gel electrophoreses. 1% gel was made with 1 g ultrapure agarose in 50 mL 1X TAE Buffer. After 15-20 min the gel had set. For gel electrophoresis analysis, 3 µL GeneRuler DNA Ladder Mix was added into well number 1. 12 µL of the sample was added to the remaining wells.

Ultrapure water was used as negative control, and the two positive controls were DNA from 5XFAD and WT with known genotype. 130 V for 15-30 min was used for separation. Images of the gels were taken using the BioRad GelDoc Go system.

2.4 EZM

The EZM is a commonly used test for unconditioned anxiety where mice are placed on a circular dark gray platform (60 cm in diameter) constructed of aluminum and divided into four equal quadrants elevated 50 cm above the floor (35). Anxious animals tend to spend more time in the enclosed sections and less time in the open sections (34). WT and 5XFAD mice were placed headfirst towards an enclosed area in the maze and filmed with a camera for 5 min before they were returned to their home cage. The ANY-Maze video tracking system (Stoelting, IL, USA) was used to record the amount of time spent in the open vs. closed zones.

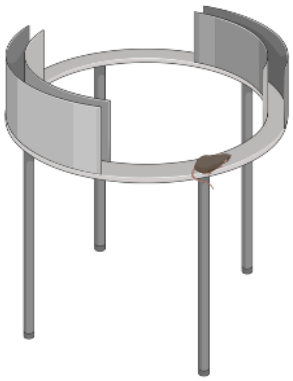

Fig. 4. The EZM. Mice are placed head first into a closed zone and allowed free exploration of the maze. Figure made in BioRender.

2.5 IF

To prepare brain tissue for IF analyzes mice were given a lethal injection of ZRF and transcardially perfused. Briefly, the chest cavity was opened, and a needle was injected into the left ventricle of the heart. To keep the needle in place a clamp was used. Going forward an incision was made to the right atrium, and the mouse was perfused by using 30 mL ice cold phosphate-buffer saline (PBS; 0.1M, pH 7.2). Then the mice were further perfused with 30 mL

ice cold paraformaldehyde (PFA). The brain was dissected out, and it was post-fixated in 4% PFA for 24 hours before sucrose (30%) treatment to prevent cells from bursting during freezing. When the brain sinks to the bottom of the tube in the sucrose solution it is ready to be frozen. The brains were then embedded in O.C.T. compound (WVR Chemicals), a mounting medium for cryosectioning before they were snap-frozen in liquid nitrogen and stored at -80°C. A NX70 cryostat (Thermo Scientific) was used to serially cut 30 μm thick coronal sections and placed on Superfrost adhesion slides (Epredia USA).

IF is a technique, which detects and locates antigens in any tissue and cell type, using immunohistochemistry and fluorescence microscopy. Fixed samples are stained with specific primary antibodies and secondary antibodies tagged with fluorophores (36). IF was performed according to Abcam staining protocol (37). Briefly, sections were washed 3 x 5 min in PBS with 0.025% Triton-X100 (TPBS). Sections were then blocked in 10% normal goat serum (NGS) with 1% bovine serum albumin (BSA) in TPBS for 1 hr at room temperature. Primary antibodies were diluted in TPBS with 1% BSA and incubated overnight at 4°C. The following primary antibodies were used: rabbit anti-amyloid beta 1-42 (1:1000, cat.nr #44-344, Invitrogen), a marker for Aβ pathology and rabbit anti-Iba1 (1:1000, cat.nr #019-19741, Wako/Fujifilm), a glial marker. After overnight incubation with primary antibody solution, sections were washed 3 x 5 min in TPBS at room temperature and incubated for 1 hr with secondary antibody solution in TPBS with 1% BSA. The following secondary antibodies were used: Alexa fluor 594 goat anti-mouse (1:1000, cat.nr #A11005, Invitrogen) and Alexa fluor 488 goat anti-rabbit (1:1000, cat.nr #A11034, Invitrogen). Sections were washed 3 x 5 min in Tris-buffered saline and coverslips were mounted using Vectashield antifade mounting medium with DAPI (cat.nr #H-1200, Vector Laboratories).

Images were taken on a widefield microscope (Zeiss Axio Observer.Z1, Germany) with Zen Pro 3.1 Software and a Hamamatsu Orca Flash 4.0 digital camera (Hamamatsu Photonoics, Japan). The same settings were used across all samples when imaging. Finally, images were post-processed in Fiji/ImageJ (Version 2.9.0/1.53t, NHI, USA) to adjust contrast and brightness.

2.6 Isolation of exosomes

Mice were anesthetized with ZRF cocktail (0.1 mg/10 g bodyweight) (see appendix A.4) injected intraperitoneally. To check that there was no pain response, the feet/tail of the mice were pinched. Then, whole blood was withdrawn using a 25 G syringe from each mouse through cardiac puncture into EDTA-coated collection tubes. The samples were then centrifuged twice at 2000 g, for 15 min at 4°C. The plasma supernatant was transferred to a new tube and stored at -80°C for exosome isolation.

Exosomes were isolated from mouse blood plasma through SEC using qEV/35nm Single Gen2 columns (Izon Science Ltd, New Zealand). Containing an agarose resin filter, the columns can isolate components of sizes from 35 to 350 nm. SEC separates molecules based on their size and has successfully been used for small-scale analysis of EVs. The isolation is efficient for EVs larger than the pore size of the matrix used, and the isolation time is short. However, it is not possible to rule out contaminations of lipoproteins of the same size as the EVs (38).

First, all plasma samples were centrifuged at 10 000 g for 10 min at 4°C to remove any cells and large particles. Then, 150 µL plasma was loaded onto a single-use column, and when all the plasma had gone into the loading frith, 2 mL freshly filtered (0.22 µM) PBS was loaded onto the column. Using an automated fraction collector V2 (Izon Science Ltd New Zealand), a total of 4 fractions were collected into new 1.5 mL Eppendorf tubes and stored at -80°C.

2.7 Characterization of exosomes

2.7.1 Nanoparticle tracking analysis (NTA)

NTA was performed on the isolated exosomes with the NanoSight NS500 and NTA3.4 software. NTA utilizes properties of both light scattering and Brownian motion to obtain the size and number of exosomes in the samples (39). Briefly, exosomes were diluted 1:100 in 0,02 µm filtered PBS and loaded into the sample chamber, illuminated by a laser beam. Particles in the path of the beam scatter the laser light which is then captured with a camera through a 20X objective. Three 60 sec videos were captured of each sample and analyzed by the software.

2.7.2 Western blot (WB)

WB is a common and valuable method for the verification and analysis of proteins, and provide further details and information regarding the target proteins (40). Advantages of WB include the possibility of using a single secondary antibody solution for the detection of multiple primary antibodies and visualization of protein bands (41). Generally, the technique can be summarized with the following steps (42):

1. Lysis of cell samples to extract protein
2. Preparation of samples
3. Prepare equipment and gels
4. Gelelectrophoresis
5. Electrotransfer onto membrane (blotting)
6. Blocking and antibody incubation
7. Imaging and visualization of bands

WB was performed after abcam general WB protocol. Fractions from exosome isolation were thawed on ice, as well as samples with cell lysate. 10x radioimmuneprecipitation assay buffer (RIPA) with protease inhibitor cocktail (PIC) was added to the samples (1:10 dilution). Samples were put on constant agitation at 4°C for 30 min and then centrifuged at 14 000 g and 4°C for 20 min.

Protein concentration

Bradford assay was performed to find the amount of protein in cell lysate and fractions.
5 ml bradford assay solution was made (see appendix A.4). The standard curve was made using the following concentrations of bovine serum albumin (BSA) in purified distilled (d)H_2O: 20 µg/µL – 10 µg/µL – 5 µg/µL - 2.5 µg/µL – 1.25 µg/µL – 0.625 µg/µL. 200 µL Bradford assay and 1 µL of RIPA was added to each well. Duplicates of the standard and triplicates of the samples were used. 1 µL of the sample was used. Negative control was dH_2O. Absorbance in the fraction sample and in the cell lysate sample was measured on PerkinElmer Victor Nivo Multimode Plate Reader. Protein concentration was calculated based on absorbance of the standard curve.

Preparation, gelelectrophoresis and blotting

One part WB sample buffer was added to 3 parts sample. The samples were denatured at 95°C for 5 min. Running buffer was made (see appendix A.4). 25 µg, 10 µg, 5 µg and 2.5 µg of the fraction sample and 2 µg of cell lysate was loaded onto wells. 5 µL of the WB ladder was used. For two membranes, A and B, a gradient gel (4-15%) with 50 µL/well (Mini-PROTEAN TGX) and a 12% gel with 20 µL/well (Mini-PROTEAN TGX) were respectively used for analysis. The gels ran at 200 V for about 30 min in the BioRad mini-Protean Tetra system with Biometra Power pack P25 T. Afterward, the gel was transferred to a membrane (Trans-Blot Turbo nitrocellulose 0.2 µm) when blotted for 3 min with a program for mini TGX on the BioRad Trans-Blot Turbo Transfer System.

Blocking and antibody incubation

After blotting, the membrane was treated with the blocking buffer (see appendix A.4) for 1 hour on agitation at room temperature. The following primary antibodies was used: β-actin (1:1000 dilution), calnexin (1:10 000 dilution), CD9 (1:500 dilution), CD63 (1:1000 dilution) and CD81 (1:1000 dilution). Primary antibody solution was made with blocking buffer and the gels was treated with the solution at 4°C overnight. The membrane was then washed with 1X TBST Tween 0.1% solution (see appendix A.4) for 5 min on shaking, and this was repeated 3 times. The secondary antibody solutions were made with blocking buffer and the following secondary antibodies; Goat-anti-Rabbit HRP (1:10 000 dilution) and Donkey-pAB-to mouse HRP (1:10 000 dilution). The membranes were incubated with the secondary antibody solutions for 1h. The membrane was then washed with 1X TBST Tween 0.1% solution for 5 min on shaking, and this was repeated 3 times.

Imaging and visualization of bands

The signal was developed using femto substrate. Even volumes of the solutions in the femto substrate kit were mixed, and 200 µL of the mix was pipetted onto the membrane. A film surrounding the membrane was used to avoid spillage. Images were taken using the BioRad GelDoc Go system.

2.7.3 TEM

Being a high-resolution microscopy method, TEM can be utilized for imaging and examining EVs. TEM is an established method when deciding the purity and quality of samples containing EVs due to its ability to differentiate between EVs and non-EV particles (43).

Formvar/carbon supported 100 mesh hexagonal copper grids (Electron Microscopy Sciences, Hatfield, PA) were places on top of 5µl drops EV-solution for 5 min followed by 3 washes on drops of dH_2O before incubation on drops of 2% methylcellulose containing 0.3% uranyl acetate for 10 min on ice. Surplus of methylcellulose-uranyl acetate was removed using a filter paper and the grids were air dried before examination using a Tecnai G2 Spirit TEM (FEI, Eindhoven, The Netherlands) equipped with a Morada digital camera using RADIUS imagining software. Images were processed using Adobe Photoshop.

2.8 Isolation of RNA from exosomes

For the isolation of RNA from exosomes, the KingFisher™ Duo Prime Purification System with a 12-tip magnetic head (Thermo Fischer Scientific cat. nr. 5400110) and NAxtra™ nucleic acid extraction kit (Lybe Scientific) was used. Two well-plates were prepared by pipetting the following solutions, one column per sample to be extracted:

Table 1. Solutions added to plate A.

Row	Reagent	Volume (µL)
C	Isopropanol	400
D	80% ethanol	400
E	80% ethanol	400
F	Ultrapure water	50

Table 2. Solutions added to plate B.

Row	Reagent	Volume (µL)
C	Isopropanol	400
D	80% ethanol	400
E	80% ethanol	400

To row B in plate A, 200 µL Naxtra Lysis Buffer and 200 µL sample from exosome isolation (fractions 1, 2, 3, and 4) were added. After mixing, 600 µL Naxtra Magnetic Beads Mix (see appendix A4) was added. A 12-tip comb was inserted into row A, and the plate was run on the program "Fast Release".

The plate was incubated for 12 min at room temperature. Afterwards, 50 µL DNase Mix (see appendix A.4) was added to each well with eluted solution. The solutions were mixed by pipetting and incubated for 10 min at room temperature.

200 µL Naxtra Lysis Buffer was added to row B in plate B. After incubation the elution solution from plate A were transferred to row B in plate B. 400 µL isopropanol was added to the same row. A 12-tip comb was added to row A, and 50 µL ultrapure water was added to an elution strip. The reaction was run on the program "Fast Strip" for 15 min.

2.9 Isolation of RNA from brain tissue

RNA from brain tissue was isolated with Qiagen RNeasy Plus Micro Kit. First, the brain tissue samples were homogenized and lysed in MD Lysing Matrix 2 ml tubes with buffer RLT plus. The tubes were placed on a tissue homogenizer (Bertin Technologies Precellys 24) at 5500 rpm for 30 sec. Supernatant was transferred to genomic (g)DNA eliminator spin column and centrifuged for 30 sec at 10 000 g. 350 µL of 70% ethanol was added to the flow-through, the sample was transferred to a RNeasy MinElute spin column and centrifuged for 15 sec at 10 000 g. After discarding the flow through, 700 µL of buffer RW1 was added to the column and centrifuged at 15 sec at 10 000 g. The flow-through was discarded, 500 µL of buffer RPE was added and the column was centrifuged at 15 sec at 10 000 g and the flow-through was discarded. 500 µL of 80% ethanol was added, the sample was centrifuged for 2 min at 10 000 g and the collection tube was discarded. After placing the column in a new collection tube (2 ml), the

column was centrifuged at 13 400 g for 5 min and the collection tube was discarded. The column was placed in a new collection tube (1.5 ml), 14 µL RNase-free water was added and the sample was centrifuged for 1 min at 13 400 g.

2.9.1 NanoDrop and Qubit concentration measurements

RNA concentration and purity were measured on Nanodrop (Thermo Scientific NanoDrop One). NanoDrop can quickly measure concentrations of DNA, RNA, and proteins in ng/µl using UV light and spectrophotometry. Measuring absorption, the purity of the sample can be given from the A260/280 value, which is defined as absorbance at 260 nm divided by absorbance at 280 nm (Thermo Fischer Scientific).

Qubit (Invitrogen Life Technologies Qubit 3.0) with two different protocols, HS Assay Kit and microRNA Assay kit, were also used to measure RNA concentration. Being fast, specific, and sensitive, the Qubit uses fluorescent dyes for concentration measurement. This method can distinguish between intact and degraded RNA, and measuring the adsorption of the sample the concentration is given in ng/µl (Thermo Fischer Scientific). All reagents for the Qubit measurements comes with the kit. Working solution was made by diluting the reagent in buffer (1:200). Two standards were made with 190 µL working solution and 10 µL of standard, and samples were made with 199 µL working solution and 1 µL sample. After incubating for 2 min the standards and samples were read with Qubit.

2.9.2. TapeStation RNA analysis

Purity of the samples were also measured on TapeStation (Agilent TapeStation 4150) following the Agilent RNA ScreenTape Assay operating procedure. TapeStation is an automated gel electrophoresis solution where the quality of samples containing RNA or DNA can be measured (Agilent Technologies).

5 µL RNA sample buffer and 1µL RNA ladder was added to the first position of the tube strip. For each sample, 5 µL RNA Sample Buffer and 1 µL RNA sample was added to the tube strip. The samples were denatured at 72°C for 3 min, placed on ice for 2 min and then spun down for 1 min. The software (Agilent TapeStation Controller) was launched, the RNA ScreenTape

device flicked and inserted into the instrument. The samples were loaded into the instrument before the analyzes was started.

2.10 RT-qPCR

RT-qPCR reaction allows real-time monitoring of PCR product formed during the progression of the reaction (44). Often used for the investigation of gene expression, the method can, as well as being sensitive, detect a large range of DNA concentrations. Another advantage of RT-qPCR is the possibility of simultaneous quantification and analysis of multiple samples (45). Detection of the reaction products usually involves the usage of fluorescent molecules, like SYBR green. SYBR green is simple, cheap, and can bind to any double-stranded DNA (46).

The isolated RNA was reverse transcribed to complementary (c)DNA with the Qiagen Quantitect Reverse Transcription Kit. RT allows for amplification of RNA into cDNA before running the RT-qPCR analysis (47). All samples and reagents were kept on ice. First, gDNA was eliminated from the sample RNA with gDNA Wipeout mastermix (see appendix A.4) and template RNA. The tubes were incubated at 42°C for 3 min. Then RNA was reverse transcribed to cDNA, then RT mastermix (see appendix A.4) was added to each tube. The samples were incubated at 42°C for 15 min, then at 95°C for 15 min to inactivate the Quantiscript Reverse Transcriptase enzyme. All cDNA samples were diluted to 2.5 ng/µL. Mastermix for the housekeeping genes, *U6* and *Gapdh* and the target genes, *Rny1* and *Rny3*, was made with SYBR green RT-qPCR mastermix (see appendix A.4). 9 µL of master mix and 1 µL of the sample were added to each well. Triplicates of all samples were used for each target. Tissue from mouse testis was used as a positive control, and the master mix with dH_2O instead of the sample was used as a negative control.

RT-qPCR was performed using the comparative method of relative quantitation in StepOne™ v2.1 Software with StepOnePlus Real-time PCR system (Applied Biosystems, USA). The results were analyzed using the Comparative C_T Method ($\Delta\Delta C_T$ Method).

Results from RT-qPCR can be processed and interpreted, for example using the comparative cycle threshold method ($\Delta\Delta C_T$). Fold change is defined as the expression of a gene in the

experimental group divided by the expression of a gene in the control group (48). The Cycle Threshold (C_T) value is defined as the cycle number when detection of fluorescence reaches a certain level (49). The $\Delta\Delta C_T$ method is based on normalizing gene expression of a target gene using values from a reference gene, thus getting the relative expression. Usually, this reference gene is a housekeeping gene, like glyceraldehyde 3-phosphate dehydrogenase (GAPDH) or β-actin. Using the following equation (I), where CT_D and CT_B is target gene expression and CT_C and CT_A is reference gene expression, the relative fold change of a target gene normalized to a reference gene can be calculated (49):

$$\Delta\Delta CT = \Delta CT(a\ target\ gene) - \Delta CT(a\ reference\ gene) = (CT_D - CT_B) - (CT_C - CT_A) \quad \text{(I)}$$

2.11 Statistics

All data were analyzed by GraphPad Prism Version 9 (GraphPad, USA). The data were first checked for statistical outliers by using the ROUT method. Data are presented as mean ± standard deviation (SD). Ordinary two-way ANOVA, with a Sidak or Tukey's multiple comparisons test, was used to compare WT and 5XFAD mice across time.

3. Results

In this project, underlying pathological mechanisms of AD were investigated. Further, we aimed to analyze levels of yRNA in exosomes and brain tissue isolated from 5XFAD and WT mice to see if there is a yRNA profile that can be used as a biomarker for AD.

3.1 Assigning mice to experimental groups with genotyping

Since we were interested in investigating the effect of AD on yRNA levels in plasma exosomes, all mice were genotyped to assign each animal to the correct experimental group. Results from genotyping showed two bands for 5XFAD mice and one band for WT mice. 5XFAD and WT share a gene at 216 bp, while 5XFAD have additional mutations, at 129 bp, causing the formation of a second band.

An example of a result from the genotyping is presented in figure 5, showing bands at expected lengths. The gel includes six wells; 1) DNA ladder; 2) negative control; 3) WT positive control; 4) 5XFAD positive control; 5) mouse 1 with unknown genotype; and 6) mouse 2 with unknown genotype. After genotyping mouse 1 was assigned to 5XFAD group and mouse 2 was assigned to WT group.

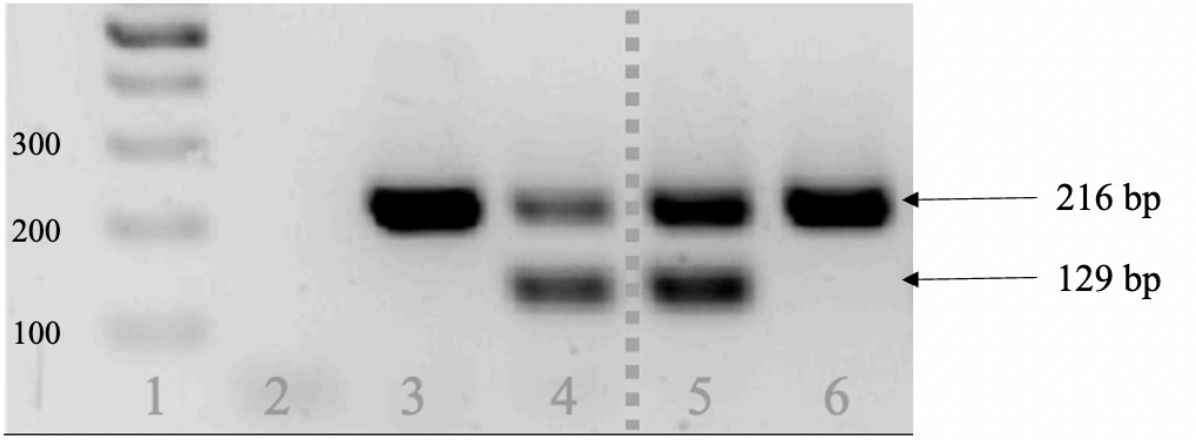

Fig. 5. Genotyping of 5XFAD and WT mice. Ladder (1), dH_2O as a negative control (2), and WT (3) and 5XFAD (4) as positive controls. DNA from two mice to be genotyped are in wells 5 and 6. Size of ladder bands are shown on the right given in bp. The gel shows bands at expected lengths.

3.2 Cognitive effects of AD

The EZM tests for anxiety-like behavior, a symptom of AD pathology, in mice. Therefore, 5XFAD mice are expected to spend less time in open zones. A two-way ANOVA with Sidak's multiple comparison test did not show any significant statistical differences between the WT and 5XFAD group across time. The Tukey's multiple comparisons test showed an increase in time spent in open area (sec) from WT at 1.5 months to WT at 6 months *(p* = 0,033). For ANOVA table, see appendix B.2.1.

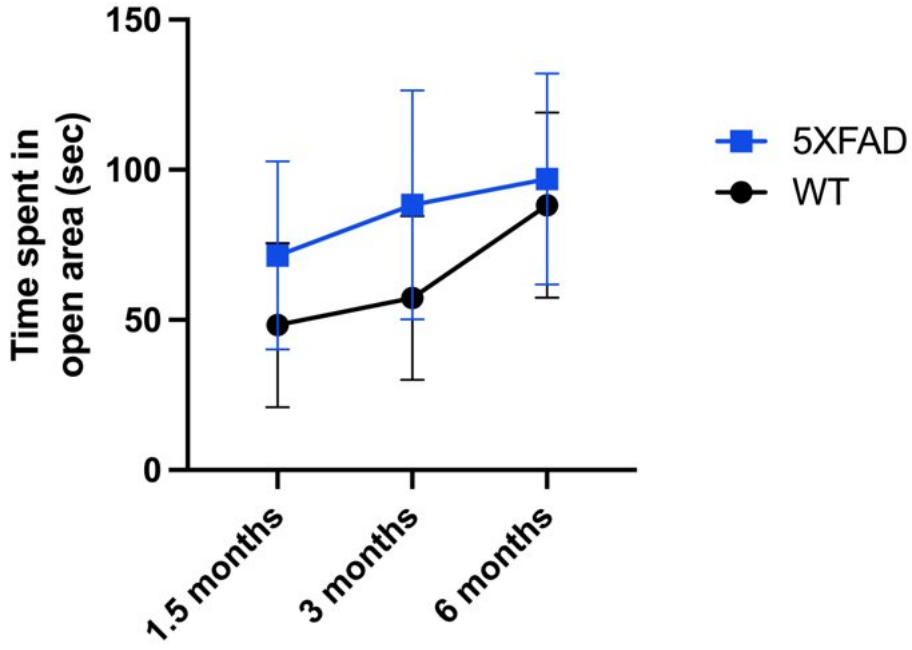

Fig. 6. Anxious behavior in mice. Time spent in open area (sec) for WT and 5XFAD mice at ages 1.5, 3, and 6 months when preforming EZM test. Data are presented as mean ± SD. Two-way ANOVA with Sidak test did not show any significant difference, and two-way ANOVA with Tukey's test shows a difference between WT 1.5 and 6 months.

3.3 AD pathology is present in 5XFAD mice

Using IF, Aβ42 was found in 5XFAD brains and not in WT brains (Fig. 7). The accumulation of Aβ in the 5XFAD brain increases over time, which can be seen in figure 7 (green specks represent Aβ42). The marker for Aβ42 visualizes accumulation of Aβ in the cortex of the brain. DAPI was used to visualize cell nuclei.

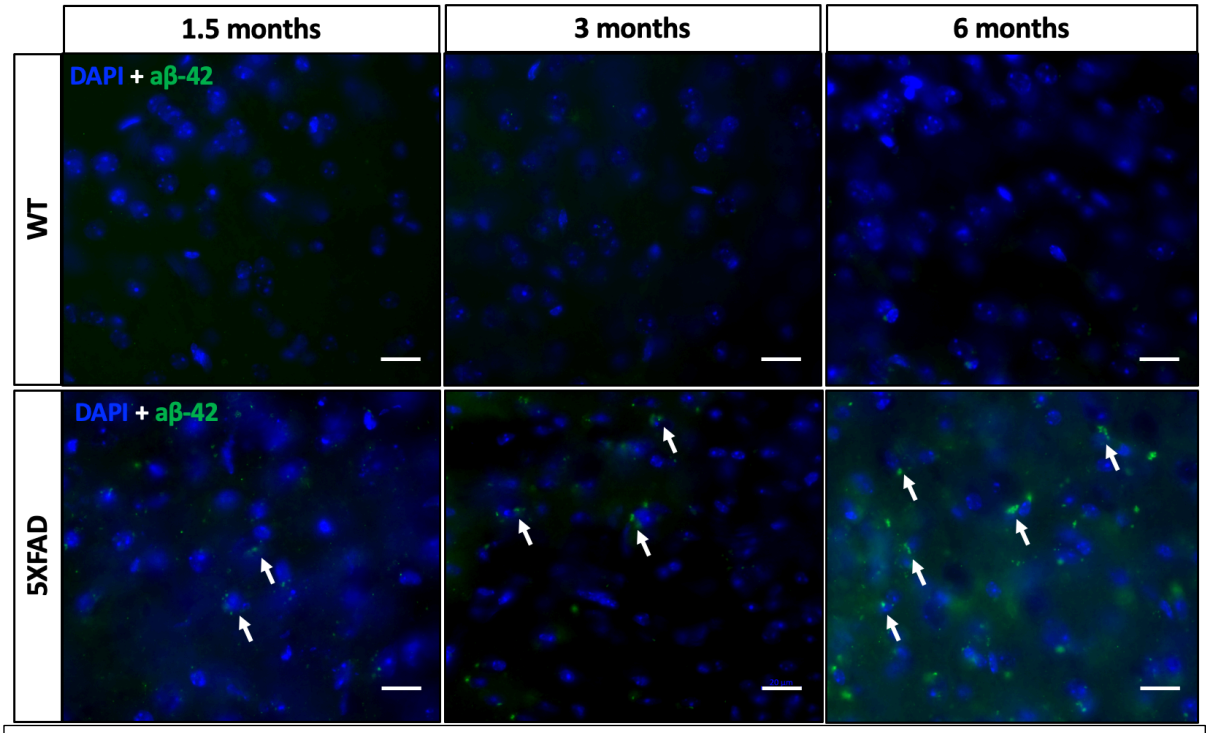

Fig. 7. AD pathology increases over time in 5XFAD mice. A marker for Aβ42 (green) was used to visualize protein accumulation in the cortex of 5XFAD and WT mice. In the 5XFAD group there is an increase in Aβ42 (seen as green specks) from 1.5 months to 6 months compared to WT mice (n = 1 in each group)*, where there is no positive staining for Aβ42 at any time point. Cell nuclei are visualized with DAPI (blue). Scale bar = 20 µm.*

Staining for microglia show Iba1+ cells in both WT and 5XFAD group (Fig. 8), but the number of microglia cells seems to increase only in the 5XFAD group which is expected. Cell nuclei were visualized with DAPI.

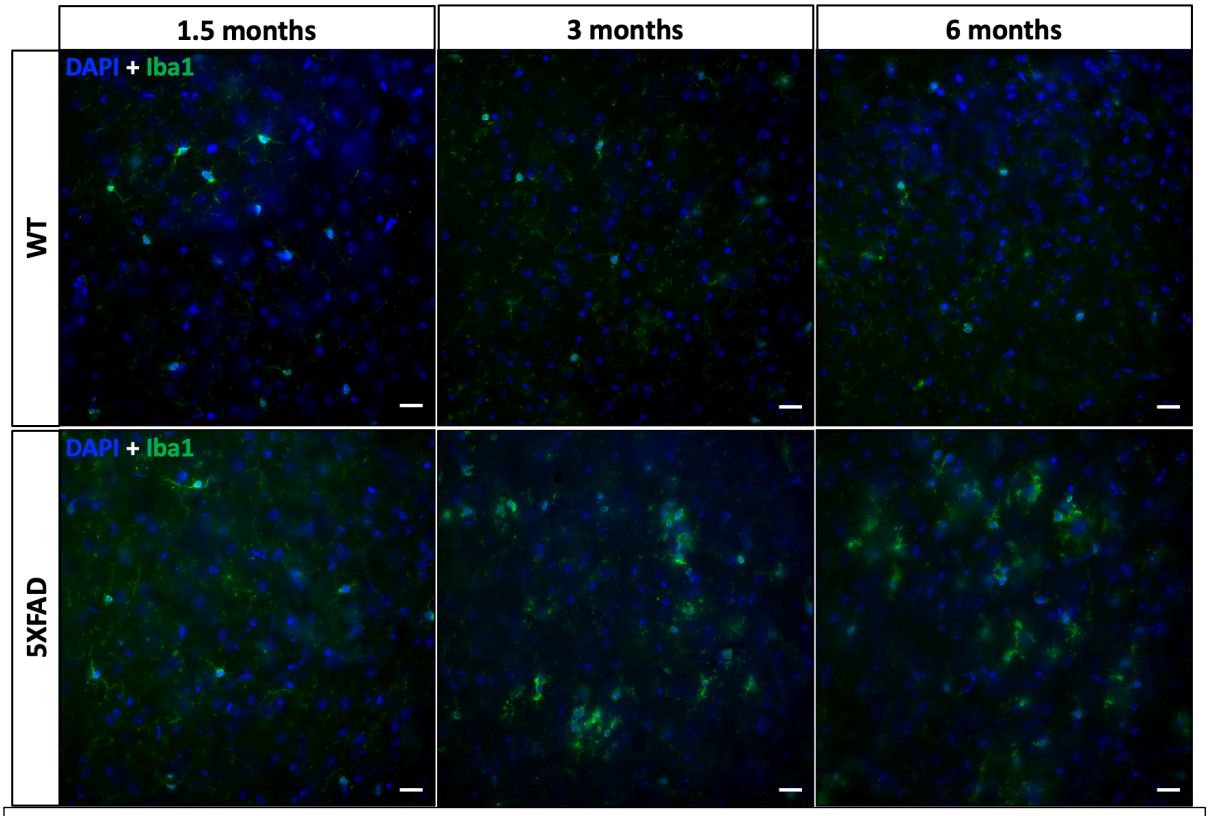

Fig. 8. Inflammation increases in the brains of 5XFAD mice with age. Iba1, a marker for endogenous inflammatory cells in the brain was used to visualize microglia (green). There is an increase in the number of microglia in the cortex of 5XFAD mice from 1.5 months of age to 6 months of age compared to WT mice (n = 1 in each group). *Cell nuclei are visualized with DAPI (blue). Scale bar = 20 µm.*

3.4 AD might affect size and number of plasma exosomes

The presence of isolated exosomes from blood plasma needs validation in case of contaminating particles, such as lipoproteins, that are of the same size as exosomes. NTA was performed on plasma exosomes after isolation to determine the size and the number of particles in the different samples. The size of the particles is concentrated around 150 nm in both the WT and 5XFAD group, but no clear size profile can be determined based on the plots.

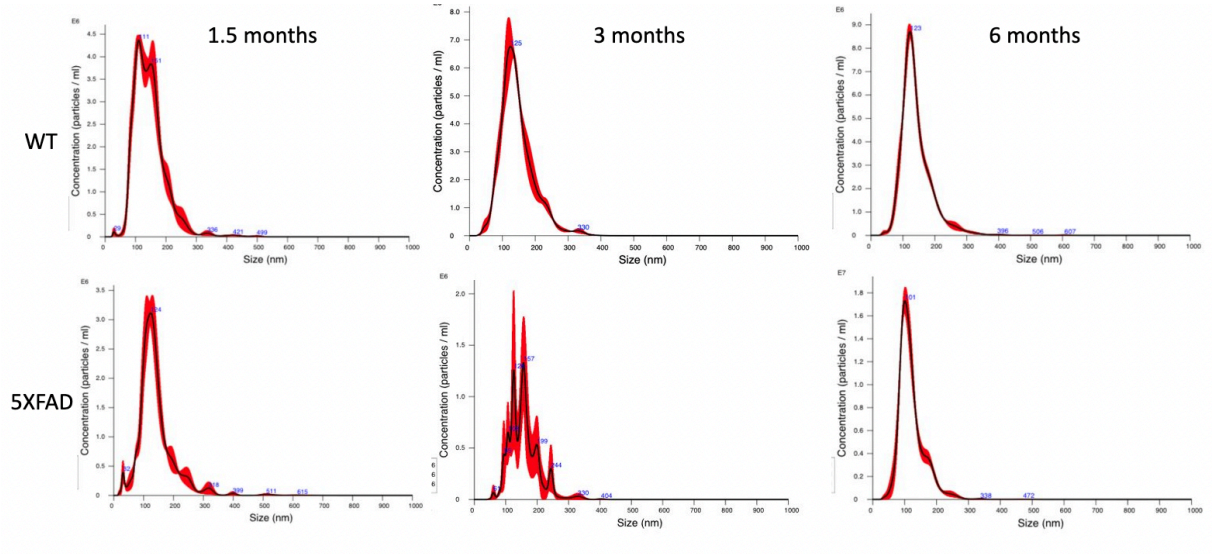

Fig. 9. NTA of samples from 1.5 months, 3 months, and 6 months old WT and 5XFAD mice. Plots show the concentration (particles/ml) as a function of size (nm) of exosomes from one representative mouse per group per time point.

Further, to compare the size of the particles in the exosomal fractions between the genotypes WT and 5XFAD, an ordinary two-way ANOVA with Sidak's multiple comparisons test was performed which showed a significant difference between WT and 5XFAD only at 3 months (Figure 10). A Tukey's multiple comparisons test was then used to analyze the size of exosomes within the same group over time, which showed that the size of isolated plasma exosomes is significantly larger in the 5XFAD group at 3 months compared to 1,5 and 6 months. For ANOVA table, see appendix B.2.2.

Finally, an ordinary two-way ANOVA showed no significant differences between the WT and 5XFAD group in the number of isolated plasma exosomes at any time point (Figure 10). However, there is a significant increase in the number of particles at 6 months in WT mice compared to 1.5 months. For ANOVA table, see appendix B.2.3.

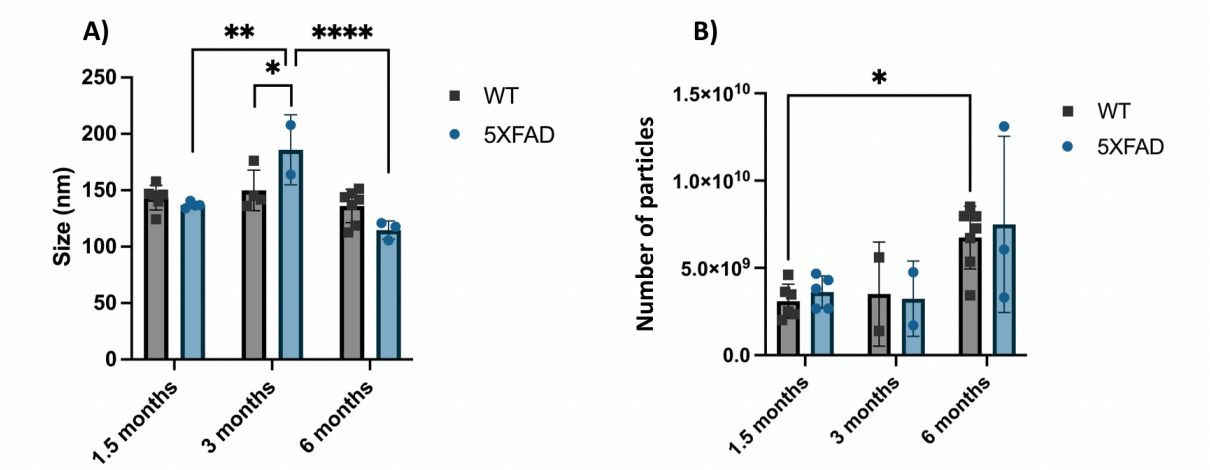

*Fig 10. NTA of isolated exosomes. A) Size of particles in samples with isolated exosomes found with NTA. The graph shows the size of particles in samples from both WT and 5XFAD at 1.5, 3 and 6 months. Data are presented as mean ± SD. Ordinary two-way ANOVA with Sidak multiple comparisons test to analyze the size of exosomes between groups at the different time points, and Tukey multiple comparisons test was used to analyze the size of exosomes within the same group over time. B) Number of particles in samples with isolated exosomes found with NTA. Data are presented as mean ± SD. The graph shows the number of particles in samples from both WT and 5XFAD at 1.5, 3 and 6 months. Data in A) and B) are presented as mean ± SD. Ordinary two-way ANOVA with Tukey test was used to analyze the number of exosomes within the same group over time. * = $p < 0.05$, ** = $p < 0.01$ and **** = $p < 0.0001$.*

100 nm control beads were used to ensure that the readouts were as correct as possible (Appendix B.1).

3.5 Analysis of membrane proteins was not successful

To further validate that the particles isolated from blood plasma are exosomes, WB was performed. To ensure equal loading of samples, concentrations of samples was normalized. A Bradford Assay was performed to measure the protein concentrations in both plasma exosome fraction samples and cell lysate. The protein amount was measured to be 0.681 µg/µL in the fraction sample and 4.19 µg/µL in the cell lysate sample.

Isolated plasma exosomes were analyzed for presence of membrane proteins by labelling the blots with exosomal transmembrane markers CD9, CD63 and CD81, and β-actin as a positive control and reference protein. We only saw expected and clear bands of β-actin (at about 42 kDa) and CD9 (at about 24 kDa) in the cell lysates (Figure 11a; well 4 and 11b; well 3, respectively). Only a smear was detected in the plasma exosomes. However, no specific bands

were detected for antibodies corresponding with either CD63, CD81 or calnexin in cell lysate or sampl

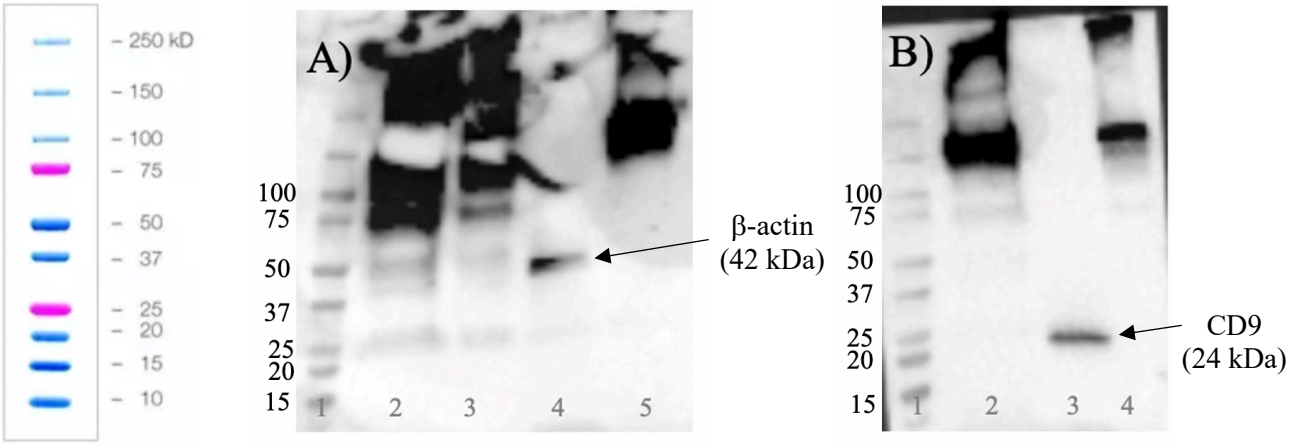

Fig. 11. WB with ladder. Samples in both blots refers to fractions of exosomes isolated from murine plasma. In A) well 1 contains ladder, well 2 contains 25 µg sample, well 3 contains 10 µg sampl ll 4 contains 2 µg cell lysate, well 5 contains 2.5 µg sample. Blot A) is stained for β-actin. In B), well 1 contains ladder, well 2 contains 25 µg sample, well 3 contains 2 µg cell lysate and well 4 contains 5 µg sample. Blot B) is stained for CD9. Ladder with size markers to the left.

3.6 Confirming presence of exosomes with TEM

TEM was performed to visualize plasma-derived exosomes in our isolated samples. The results show the presence of particles with the expected size and morphology in the WT group (Figure 12a) and in the 5XFAD group (Figure 12b).

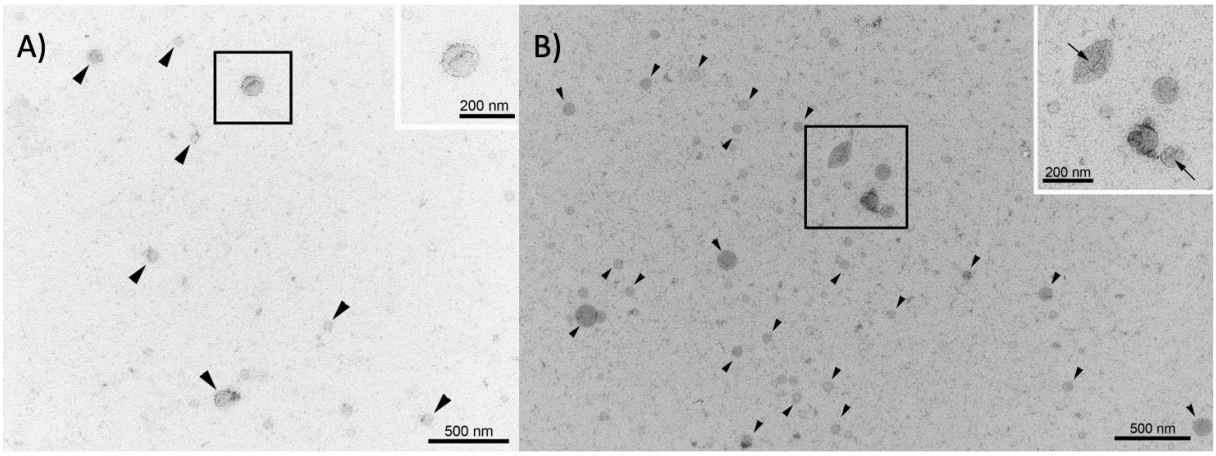

Fig. 12. TEM images of isolated EVs. In both A) for WT and B) for 5XFAD, EVs of various size are indicated by arrowheads. The characteristic cup shape of collapsed vesicles is indicated by arrows in the insert which represents enlargement of the framed area.

3.7 AD affects Rny3 levels in brain tissue of 5XFAD mice in the early stages of AD

RT-qPCR was performed to look at the levels of *Rny1* and *Rny3* in plasma exosomes and mouse brain tissue. In the plasma exosome samples we tested, there was no detection of *Rny1* or *Rny3,* results are therfore not shown. There was no detection of the reference gene either.

A two-way ANOVA with Sidak's multiple comparison test was performed to look at possible differences in *Rny3* levels in brain tissue between the WT and 5XFAD group. The results show a significant difference between WT and 5XFAD group at 1.5 months, but not at later time points. The *Rny3* levels were higher in the 5XFAD group. Gene expression of *Rny3* over time, within the same genotype, was analyzed using a two-way ANOVA with Tukey's multiple comparisons test, which showed a significantly lower level of *Rny3* at 3 and 6 months compared to 1.5 months in the 5XFAD group. The level of *Rny3* did not change in the WT group at any time point. There was no detection of *Rny1* in the brain tissue, results are thefore not shown. For ANOVA table, see appendix B.2.4.

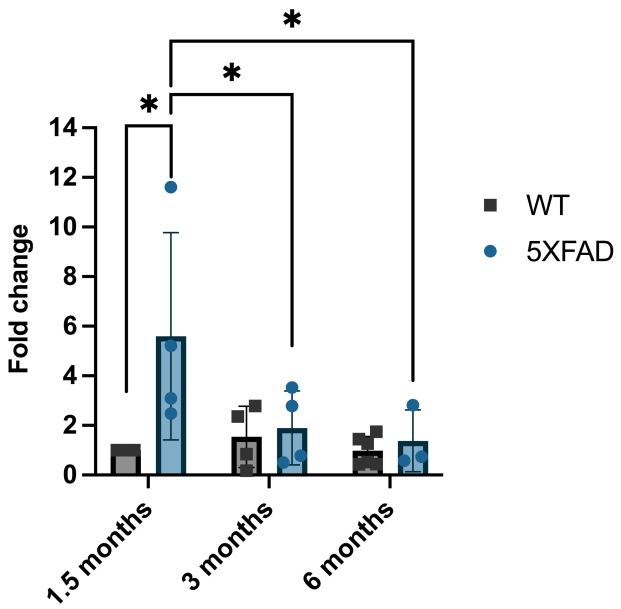

*Fig. 13. Rny3 expression in brain tissue for 5XFAD vs WT at 1.5, 3 and 6 months normalized to reference gene Gapdh. Data are presented as mean ± SD. Ordinary Two-way ANOVA, with Sidak multiple comparisons test was used for analysis of data of Rny3 gene expression between genotypes. Analysis of Rny3 gene expression data within the same genotype, over time, a two-way ANOVA with Tukey multiple comparisons tests was used. * = $p < 0.05$.*

4. Discussion

The main finding in this project is that at an early stage of disease, AD affects the level of *Rny3* in the brains of transgenic mice. Furthermore, AD affects the size but not the number of isolated plasma exosomes.

4.1 Phenotype of 5XFAD mice could not be determined with behavior test

Results from EZM showed no difference in time spent in open zones between WT and 5XFAD genotypes at the different time points. The EZM is a commonly used behavior test for unconditioned anxiety in mice, since anxiety is a common feature of AD. For 5XFAD mice a significant decrease in time spent in open zones, due to anxiety-like behavior, was expected. However, there was no change in anxiety for 5XFAD mice over time. Although the time spent in open zones was expected to not change for WT mice, a significant increase over time was found. These results highlights one of the challenges with animal research, as we expected the time spent in open areas to decrease for 5XFAD, and no change for WT. Mice are sensitive to changes in their environment (50), and we cannot rule out that external factors such as loud noises etc. may have influenced their behavior in the EZM. In addition, this study included a low number of experimental animals in some groups. If more animals had been included in the study, perhaps a stronger phenotype could have been observed.

The use of transgenic mice to model human neurodegenerative diseases is common, since the complexity of mouse brains can be compared to the complex human brain (51). In addition, the protein-coding part of genome of mice and humans are 85 percent identical (52), including the RNY1 and RNY3 genes, which supports the choice of using mice as a model in this project (51). However, the mouse model used does not present other AD pathologies than Aβ plaque pathology. The transgenic 5XFAD develop symptoms of AD at a young age, since there are five mutations which stimulates overproduction of Aβ. In humans, it is rarely mutations in the same genes that causes AD, and Aβ pathology therefore occur at an older age (8).

Images from IF show more inflammation and Aβ pathology in the brains of the 5XFAD mice compared to WT mice. Inflammation increases in the 5XFAD mouse brain with age, which

along with Aβ pathology, confirms the genotype of 5XFAD mice. The Aβ pathology and inflammation tendencies are expected in the 5XFAD mice, as AD causes inflammation and aggregation of Aβ in the brain.

4.2 Validation of exosomes

SEC is a method for isolating particles at a given size and was therefore utilized for the isolation of exosomes from murine plasma samples. Another widely used method is UC, a process that can take up to 18 hours. The isolation time when performing SEC is shorter compared to UC. In addition, SEC allows isolation of exosomes from small volumes of plasma whereas UC requires larger volumes. When extracting plasma from mice, the total volume of sample collected is around 600 μL. Studies have shown that isolating exosomes with SEC gives samples with a higher purity compared to UC (22). NTA, WB and TEM were performed using fractions containing isolated exosomes. Although WB did not validate the exosomal membrane proteins, NTA and TEM confirmed that exosomes were present in the fraction samples. This leads us to believe that the executed method is efficient for isolating exosomes.

NTA was performed to indicate whether the particles in the collected fractions are exosomes, and to study abundance of the particles in WT and 5XFAD mice. Diameters of around 40-160 nm are expected for exosomes. Results from the NTA show that the particles in the samples are in the expected size range, which indicates that there are exosomes in the sample. However, we cannot rule out that some of the particles are lipoproteins since these can have the same diameter as exosomes. TEM was used for further confirmation of the presence of exosomes. The images showed circular particles with a cup-shape that had a diameter within the interval of exosomes, 40-160 nm. This leads us to believe that the isolation of exosomes from murine plasma was successful.

The membrane proteins CD9, CD63 and CD81 can be used to validate exosomes in plasma samples, as they are present in all exosomes, and function as exosomal markers. Optimizing WB took up time during the project, as a result of defective equipment and inaccuracy in method execution. However, the results show presence of proteins in both membranes. The bands present for the exosome samples are smeared, suggesting that there is protein in the

sample, but no clear band was visible and therefore we cannot determine whether the exosome samples contain target proteins or not. These results do not contradict the fact that the samples might be abundant with exosomes, but WB alone cannot validate their presence.

During the optimization of the method, corresponding antibodies to the membrane proteins CD63 and CD81 were also used, but the results gave unspecific bands. Using calnexin as a negative control was attempted, but this only gave nonspecific bands in the cell lysate, causing results from these attempts to be discarded.

The clear bands in the positive control, cell lysate, proves correct execution of the WB method. Optimizing the sample preparation for exosomes could have given more clear results, but there was not enough time in the scope of the project to finish the optimization.

4.3 AD affects size, but not number, of isolated plasma exosomes

Results show a slight increase in size of particles from 5XFAD to WT. The only significant difference is between 5XFAD and WT at 3 months. For 5XFAD there is an increase in particle size from 1.5 months to 3 months, and a decline in size from 3 months to 6 months. The size of particles in WT seems to be approximately the same at all time points. The increase in size of exosomes in 5XFAD mice at 3 months in comparison to the stability of size of particles in WT over time leads us to believe that AD affects the size of the particles.

The number of plasma exosomes was also studied using NTA. Results showed an increase in number of plasma particles in WT mice from 1.5 months to 6 months. The increase in numbers for WT was significant ($p < 0.05$) according to the ANOVA test. There was also an increase in the number of exosomes at 6 months in the 5XFAD group, although not significant. This might indicate that normal aging in mice can increase number of exosomes in plasma. Since there was no difference between WT and 5XFAD group at any time point this suggests that AD does not affect the number of plasma particles. Recent studies on the effect AD can have on both the size and number of plasma exosomes have given varied results. Some results have implied a decline in size and number, others found an increase in both properties, and some showed no change. Differences in results are likely due to variations in source of exosomes, as well as

method used for exosome isolation (53). Further research is needed to present a firm conclusion regarding how AD affects the size and numbers of particles in plasma.

4.4 AD affects the expression of Rny3 in mouse brain

A promising biomarker for AD are yRNAs, which are strongly associated with exosomes. Knowing our samples are abundant with exosomes, isolation of yRNAs from exosome samples could prove changes in yRNA gene expression due to AD pathology.

For the RT-qPCR analysis of gene expression, RNA from both brain tissue and exosomes were used. Results from gene expression analysis of murine yRNA in brain tissue showed a significant change in expression levels of *Rny3* in 5XFAD mice at early stages of the disease compared to WT mice. *Rny1* did not reach threshold detection level, indicating that the expression is too low in brain tissue in mice to be detected with RT-qPCR.

Several studies found that systemic inflammation affected expression levels of the different human yRNAs in plasma EVs (10, 54). Further, it was also found that there were cell specific changes in yRNA levels. Since AD also leads to an upregulation of inflammation in the brain, we hypothesized that a similar change in yRNA levels can be detected. There seem to be little to no change at later stages of AD, when compared to WT.

There are no results from RT-qPCR of isolated RNA from plasma exosomes. Despite a lot of effort spent on troubleshooting and optimization, *Rny1* and *Rny3* did not reach threshold detection level in the RT-qPCR. Troubleshooting included testing different housekeeping genes, this included *U6* and *Gapdh*. *U6* was found to be an unsuitable reference gene, due to too large variation in C_T values. We also tested different amounts of cDNA (from 1 to 12.5 ng per reaction). Nanodrop and Qubit was used to measure the concentration of isolated RNA from plasma exosomes, with varying results. We then tested different methods to isolate RNA. Despite getting a readout from Nanodrop, the concentration was too low to be detected on Qubit. Most likely there was not enough RNA in our samples due to the small amount of plasma that exosomes were isolated from or the methods we tested to isolate RNA were not optimal.

4.5 Conclusion and future perspectives

Although the EZM test did not show any significant difference between WT and 5XFAD mice, we show that there is presence of Aβ pathology and increased inflammation. Further, there is a significant difference in yRNA levels in brain tissue between 5XFAD and WT mice at 1.5 months. AD does not affect the number of plasma exosomes since there is no difference between the two groups at different time points. Although only significant for the WT group, the results from NTA analysis does suggests that the number of exosomes increases with age in the mice. Inflammation has been shown to increase in mice as they grow older (55), which might affect the number of exosomes. Studies on ways to differentiate types of exosomes and standardize exosome extraction, isolation and characterization can help future methods for diagnostics.

There was not enough time in the scope of this project to finish optimizing all the methods used for exosomes, and both WB and RT-qPCR with exosome samples needs to be optimized. Another interesting factor to look at in relation to exosomes and yRNA in AD, is fragmentation of yRNAs, since previous studies have shown increased fragmentation in different disease models. Further, it would be interesting to study the effect inflammation has on yRNA and exosomes. The project has opened new ideas on what to look at in the future, and hopefully it is possible to find a yRNA profile which can be used as a biomarker for AD.

References

1. Gale SA, Acar D, Daffner KR. Dementia. Am J Med. 2018;131(10):1161-9.
2. Moyle W. The promise of technology in the future of dementia care. Nat Rev Neurol. 2019;15(6):353-9.
3. Mattson MP. Pathways towards and away from Alzheimer's disease. Nature. 2004;430(7000):631-9.
4. Lane CA, Hardy J, Schott JM. Alzheimer's disease. Eur J Neurol. 2018;25(1):59-70.
5. Hampel H, Hardy J, Blennow K, Chen C, Perry G, Kim SH, et al. The Amyloid-β Pathway in Alzheimer's Disease. Molecular Psychiatry. 2021;26(10):5481-503.
6. Beason-Held LL, Goh JO, An Y, Kraut MA, O'Brien RJ, Ferrucci L, et al. Changes in brain function occur years before the onset of cognitive impairment. J Neurosci. 2013;33(46):18008-14.
7. Wyss-Coray T. Ageing, neurodegeneration and brain rejuvenation. Nature. 2016;539(7628):180-6.
8. Oakley H, Cole SL, Logan S, Maus E, Shao P, Craft J, et al. Intraneuronal β-Amyloid Aggregates, Neurodegeneration, and Neuron Loss in Transgenic Mice with Five Familial Alzheimer's Disease Mutations: Potential Factors in Amyloid Plaque Formation. The Journal of Neuroscience. 2006;26(40):10129-40.
9. Rembach A. The search for a blood-based biomarker for Alzheimer disease. Nature Reviews Neurology. 2014;10(11):618-9.
10. Varesi A, Carrara A, Pires VG, Floris V, Pierella E, Savioli G, et al. Blood-Based Biomarkers for Alzheimer's Disease Diagnosis and Progression: An Overview. Cells. 2022;11(8).
11. Institute NC. Biomarker. NCI Dictionary of Cancer Terms.
12. Aronson JK, Ferner RE. Biomarkers-A General Review. Curr Protoc Pharmacol. 2017;76:9.23.1-9..17.
13. Blennow K, Zetterberg H. Biomarkers for Alzheimer's disease: current status and prospects for the future. Journal of Internal Medicine. 2018;284(6):643-63.
14. Dhiman K, Blennow K, Zetterberg H, Martins RN, Gupta VB. Cerebrospinal fluid biomarkers for understanding multiple aspects of Alzheimer's disease pathogenesis. Cell Mol Life Sci. 2019;76(10):1833-63.
15. Hornung S, Dutta S, Bitan G. CNS-Derived Blood Exosomes as a Promising Source of Biomarkers: Opportunities and Challenges. Frontiers in Molecular Neuroscience. 2020;13.

16. Hampel H, Shaw LM, Aisen P, Chen C, Lleó A, Iwatsubo T, et al. State-of-the-art of lumbar puncture and its place in the journey of patients with Alzheimer's disease. Alzheimers Dement. 2022;18(1):159-77.
17. Thompson AG, Gray E, Heman-Ackah SM, Mäger I, Talbot K, Andaloussi SE, et al. Extracellular vesicles in neurodegenerative disease — pathogenesis to biomarkers. Nature Reviews Neurology. 2016;12(6):346-57.
18. Tkach M, Théry C. Communication by Extracellular Vesicles: Where We Are and Where We Need to Go. Cell. 2016;164(6):1226-32.
19. Driedonks TAP, Nolte-'t Hoen ENM. Circulating Y-RNAs in Extracellular Vesicles and Ribonucleoprotein Complexes; Implications for the Immune System. Frontiers in Immunology. 2019;9.
20. Kalluri R, LeBleu VS. The biology, function, and biomedical applications of exosomes. Science. 2020;367(6478).
21. Poupardin R, Wolf M, Strunk D. Adherence to minimal experimental requirements for defining extracellular vesicles and their functions. Advanced Drug Delivery Reviews. 2021;176:113872.
22. Doyle LM, Wang MZ. Overview of Extracellular Vesicles, Their Origin, Composition, Purpose, and Methods for Exosome Isolation and Analysis. Cells. 2019;8(7).
23. Beatriz M, Vilaça R, Lopes C. Exosomes: Innocent Bystanders or Critical Culprits in Neurodegenerative Diseases. Frontiers in Cell and Developmental Biology. 2021;9.
24. Zheng D, Huo M, Li B, Wang W, Piao H, Wang Y, et al. The Role of Exosomes and Exosomal MicroRNA in Cardiovascular Disease. Frontiers in Cell and Developmental Biology. 2021;8.
25. Hall AE, Turnbull C, Dalmay T. Y RNAs: recent developments. BioMolecular Concepts. 2013;4(2):103-10.
26. Kowalski MP, Krude T. Functional roles of non-coding Y RNAs. The International Journal of Biochemistry & Cell Biology. 2015;66:20-9.
27. Hung T, Pratt GA, Sundararaman B, Townsend MJ, Chaivorapol C, Bhangale T, et al. The Ro60 autoantigen binds endogenous retroelements and regulates inflammatory gene expression. Science. 2015;350(6259):455-9.
28. Zhang X, Trebak F, Souza LAC, Shi J, Zhou T, Kehoe PG, et al. Small RNA modifications in Alzheimer's disease. Neurobiology of Disease. 2020;145:105058.
29. Godoy PM, Bhakta NR, Barczak AJ, Cakmak H, Fisher S, MacKenzie TC, et al. Large Differences in Small RNA Composition Between Human Biofluids. Cell Rep. 2018;25(5):1346-58.

30. van Balkom BWM, Eisele AS, Pegtel DM, Bervoets S, Verhaar MC. Quantitative and qualitative analysis of small RNAs in human endothelial cells and exosomes provides insights into localized RNA processing, degradation and sorting. Journal of Extracellular Vesicles. 2015;4(1):26760.
31. Sims R, Hill M, Williams J. The multiplex model of the genetics of Alzheimer's disease. Nat Neurosci. 2020;23(3):311-22.
32. Biundo F, Ishiwari K, Del Prete D, D'Adamio L. Interaction of ApoE3 and ApoE4 isoforms with an ITM2b/BRI2 mutation linked to the Alzheimer disease-like Danish dementia: Effects on learning and memory. Neurobiology of Learning and Memory. 2015;126:18-30.
33. Morris RGM. Spatial localization does not require the presence of local cues. Learning and Motivation. 1981;12(2):239-60.
34. Shepherd JK, Grewal SS, Fletcher A, Bill DJ, Dourish CT. Behavioural and pharmacological characterisation of the elevated "zero-maze" as an animal model of anxiety. Psychopharmacology (Berl). 1994;116(1):56-64.
35. Tucker LB, McCabe JT. Behavior of Male and Female C57BL/6J Mice Is More Consistent with Repeated Trials in the Elevated Zero Maze than in the Elevated Plus Maze. Front Behav Neurosci. 2017;11:13.
36. Im K, Mareninov S, Diaz MFP, Yong WH. An Introduction to Performing Immunofluorescence Staining. Methods Mol Biol. 2019;1897:299-311.
37. abcam. Immunocytochemistry and immunofluorescence staining protocol.
38. Stranska R, Gysbrechts L, Wouters J, Vermeersch P, Bloch K, Dierickx D, et al. Comparison of membrane affinity-based method with size-exclusion chromatography for isolation of exosome-like vesicles from human plasma. J Transl Med. 2018;16(1):1.
39. Auger C, Brunel A, Darbas T, Akil H, Perraud A, Bégaud G, et al. Extracellular Vesicle Measurements with Nanoparticle Tracking Analysis: A Different Appreciation of Up and Down Secretion. International Journal of Molecular Sciences. 2022;23(4):2310.
40. Counts SE. Western Blot. I: Kompoliti K, Metman LV, red. Encyclopedia of Movement Disorders. Oxford: Academic Press; 2010. s. 323-6.
41. Martins-de-Souza D, Guest PC, Vanattou-Saifoudine N, Harris LW, Bahn S. Chapter 4 - Proteomic Technologies for Biomarker Studies in Psychiatry: Advances and needs. I: Guest PC, Bahn S, red. International Review of Neurobiology. 101: Academic Press; 2011. s. 65-94.
42. Mahmood T, Yang PC. Western blot: technique, theory, and trouble shooting. N Am J Med Sci. 2012;4(9):429-34.

43. Pascucci L, Scattini G. Imaging extracelluar vesicles by transmission electron microscopy: Coping with technical hurdles and morphological interpretation. Biochimica et Biophysica Acta (BBA) - General Subjects. 2021;1865(4):129648.
44. Maddocks S, Jenkins R. Chapter 4 - Quantitative PCR: Things to Consider. I: Maddocks S, Jenkins R, red. Understanding PCR. Boston: Academic Press; 2017. s. 45-52.
45. Hoy MA. Chapter 8 - DNA Amplification by the Polymerase Chain Reaction: Molecular Biology Made Accessible. I: Hoy MA, red. Insect Molecular Genetics (Third Edition). San Diego: Academic Press; 2013. s. 307-72.
46. Cremonesi P, Monistero V, Moroni P, Barberio A, Almeida R, Latorre AA, et al. Detection Methods. I: McSweeney PLH, McNamara JP, red. Encyclopedia of Dairy Sciences (Third Edition). Oxford: Academic Press; 2022. s. 457-68.
47. Jalali M, Zaborowska J, Jalali M. Chapter 1 - The Polymerase Chain Reaction: PCR, qPCR, and RT-PCR. I: Jalali M, Saldanha FYL, Jalali M, red. Basic Science Methods for Clinical Researchers. Boston: Academic Press; 2017. s. 1-18.
48. Lal A, Roudebush WE, Mainigi M, Chosed RJ. Fluorescent-dependent comparative Ct method for qPCR gene expression analysis in IVF clinical pre-implantation embryonic testing. Biology Methods and Protocols. 2021;6(1):bpab001.
49. Rao X, Huang X, Zhou Z, Lin X. An improvement of the 2ˆ(-delta delta CT) method for quantitative real-time polymerase chain reaction data analysis. Biostat Bioinforma Biomath. 2013;3(3):71-85.
50. Farazi N, Mahmoudi J, Sadigh-Eteghad S, Farajdokht F, Rasta SH. Synergistic effects of combined therapy with transcranial photobiomodulation and enriched environment on depressive- and anxiety-like behaviors in a mice model of noise stress. Lasers in Medical Science. 2022;37(2):1181-91.
51. Goodarzi P, Payab M, Alavi-Moghadam S, Larijani B, Rahim F, Bana N, et al. Development and validation of Alzheimer's Disease Animal Model for the Purpose of Regenerative Medicine. Cell and Tissue Banking. 2019;20(2):141-51.
52. Institute NHGR. Why Mouse Matters. 2010.
53. Zou Y, Mu D, Ma X, Wang D, Zhong J, Gao J, et al. Review on the roles of specific cell-derived exosomes in Alzheimer's disease. Front Neurosci. 2022;16:936760.
54. Driedonks TAP, Mol S, de Bruin S, Peters A-L, Zhang X, Lindenbergh MFS, et al. Y-RNA subtype ratios in plasma extracellular vesicles are cell type- specific and are candidate biomarkers for inflammatory diseases. Journal of Extracellular Vesicles. 2020;9(1):1764213.

55. Thevaranjan N, Puchta A, Schulz C, Naidoo A, Szamosi JC, Verschoor CP, et al. Age-Associated Microbial Dysbiosis Promotes Intestinal Permeability, Systemic Inflammation, and Macrophage Dysfunction. Cell Host & Microbe. 2017;21(4):455-66.e4.

Appendix A

A.1 Primer sequences

Table A.1. Sequences of all primers used during the project.

Primer	Sequence (5’ -> 3’)
Gapdh F	TCGTCCCGTAGACAAAATGGT
Gapdh R	CGCCCAATACGGCCAAA
Rny1 F	GGCTGGTCCGAAGGTAGTGAG
Rny1 R	GGGGAAAGTGTAGAACAGGAG
Rny3 F	CCGAGAGTAGTGGTGTTTAC
Rny3 R	AAGCAGTGGGAGCGGAGAA
WT R	TATACAACCTTGGGGGATGG
5XFAD/WT Common F	ACCCCCATGTCAGAGTTCCT
5XFAD R	CGGGCCTCTTCGCTATTAC

A.2 List of antibodies with dilutions used in WB

Table A.2. List of antibodies used during the project, including cat. number, manufacturer and dilutions.

Anti-β–actin, 1:1000 (A1978-1000L), 42kD, Mouse	Sigma Aldrich
Anti-Calnexin, 1:10 000 (PA5-34754), 95 kD, Rabbit	Invitrogen Antibodies
Anti-CD63, 1:1000 (PA5-92370), 45kD, Rabbit	Invitrogen Antibodies
Anti-CD81, 1:1000 (MA32333), 20-25kD, Rabbit	Invitrogen Antibodies
Anti-CD9, 1:500 (10626D), 24kD, Mouse	Invitrogen Antibodies
Donkey-pAB-to mouse HRP, 1:10 000 (ab6820)	abcam
Goat-anti-Rabbit HRP, 1:10 000 (P1-1000-1)	Vector Labratories

A.3 Chemicals/solutions

Table A.3. List of all chemicals and solutions used during the project.

Chemical	***Manufacturer (kit)***
1X TAE Buffer	OUS Substrate-lab
BSA Molecular Biology Grade	BioLabs Inc.
Buffer RLT Plus	QIAGEN RNeasy Plus Micro Kit (50)
Buffer RPE	QIAGEN Rneasy Plus Micro Kit (50)
Buffer RW1	QIAGEN Rneasy Plus Micro Kit (50)
Dnase-1 Enzyme	QIAGEN Rnase-free Dnase set (250)
Ethanol	Antibac
Femto substrate - SuperSignal West Femto Maximum Sensitivity Substrate	Thermo Scientific
gDNA WipeOut Buffer	QIAGEN QuantiTect® Reverse Transcription Kit
GeneRuler DNA Ladder	Thermo Scientific
GoTaq Green	Promega
Isopropanol	EMSURE 2-propanol for analysis
dH_2O	MilliQ (Sigma Aldrich)
NaOH 1M	Sigma Aldrich
Naxtra Lysis Buffer	Lybe Scientific
Naxtra Magnetic Beads	Lybe Scientific
Paraformaldehyde PFA	Sigma Aldrich
Phosphate-buffer Saline PBS	Gibco pH 7.4

PIC 100 X	Merck
Protein Assay Dye	BioRad Protein Assay Dye Reagent Concentrate
Quantiscript Reverse Transcription	QIAGEN QuantiTect® Reverse Transcription Kit
Quantiscript RT Buffer 5 X	QIAGEN QuantiTect® Reverse Transcription Kit
Qubit microRNA Buffer	Invitrogen Qubit microRNA Assay Kit
Qubit microRNA Reagent	Invitrogen Qubit microRNA Assay Kit
Qubit microRNA Standard 1	Invitrogen Qubit microRNA Assay Kit
Qubit microRNA Standard 2	Invitrogen Qubit microRNA Assay Kit
Qubit RNA Buffer	Invitrogen Qubit RNA HS Assay Kit
Qubit RNA Reagent	Invitrogen Qubit RNA HS Assay Kit
Qubit RNA Standard 1	Invitrogen Qubit RNA HS Assay Kit
Qubit RNA Standard 2	Invitrogen Qubit RNA HS Assay Kit
RDD DNA Buffer	QIAGEN Rnase-free Dnase set (250)
Rnase-free water	QIAGEN QuantiTect® Reverse Transcription Kit
RT Primer Mix	QIAGEN QuantiTect® Reverse Transcription Kit
Skim Milk Powder	Sigma-Aldrich
PowerUp SYBR Green Master Mix	Applied BioSystems
TapeStation RNA ScreenTape Ladder	Agilent Technologies
TapeStation High Sensitivity RNA ScreenTape Sample Buffer	Agilent Technologies

Tris-HCl	OUS Substrate-lab
Tris/Glycine/SDS 10 X	BioRad
Tween 20	Merck
Ultrapure Agarose	Invitrogen
Ultrapure Water	Invitrogen
WB Ladder -Precision Plus Protein Dual Color Standards, 500µl #1610374	BioRad
WB Sample Buffer, 4X Bolt	Life Technologies

A.4 Recipes for buffers and solutions

Table A.4.1. List of chemicals used for all buffers and solutions made during the project.

Buffer/Solution	***Components***
10X RIPA	19 µL 0.1% RIPA + 1X PIC 1 µL 20% SDS
1X TBS Wash Buffer	50 mL TBS 10X + 450 dH_2O
Blocking Buffer	5 g Skim Milk Powder + 100 mL TBST Tween 0.1%
Bradford Assay Solution	4 parts dH_2O + 1 part Protein Assay Dye
DNase Mix	2.5 µL DNase-1 Enzyme + 10 µL RDD DNA Buffer + 37.5 µL H_2O
Hot Shot Buffer	7.5 mg Na_2EDTA + 2.5 mL 1M NaOH + 97.5 mL dH_2O, pH adjusted to 12.
Naxtra Magnetic Beads Mix	20 µL Naxtra Magnetic Beads 580 µL isopropanol
Neutralizing Buffer	650 mg Tris-HCL + 100 mL dH_2O, pH adjusted to 5.
Running Buffer	50 mL 10X Tris/Glycine/SDS + 950 mL dH_2O
TBS 10X	12 gr Tris + 44 gr NaCl in 200 mL MQ (pH adjusted to 7.6 with HCL)
TBST Tween 0.1%	50 mL TBS 10X + 450 mL dH_2O + 500 µL Tween 20
ZRF	18.7mg Tilamine + 0.45mg Xylazine + 2.6mg Fentanyl per mL

Table A.4.2. Solutions used for making Master Mix for PCR.

Component	***Volume/ pr sample (µL)***
GoTaq Green	6.25
dH_2O	3.55
Common Forward Primer	0.4
WT Reverse Primer	0.4
5XFAD Reverse Primer	0.4

Table A.4.3. Reagents and volumes needed for gDNA wipeout.

Component	***Volume/reaction (µL)***
gDNA Wipeout Buffer	2
Template RNA	Variable
RNase-free water	Variable
Total	14

Table A.4.4. Components and volumes of RT Master Mix.

Component	***Volume/ pr sample (µL)***
Quantiscript Reverse Transcription	1
Quantiscript RT Buffer, 5x	4
RT Primer Mix	1
Total	6

Table A.4.5. Components and volumes of PCR Master Mix.

Component	***Volume/ pr sample (µL)***
SYBR Green	5
Forward Primer	0.1
Reverse Primer	0.1
dH_2O	3.8
Total	9

Appendix B

B.1 Control beads in NTA

In figure B.1 the concentration and size measured using NTA of a control test of beads with a diameter of 100 nm is shown.

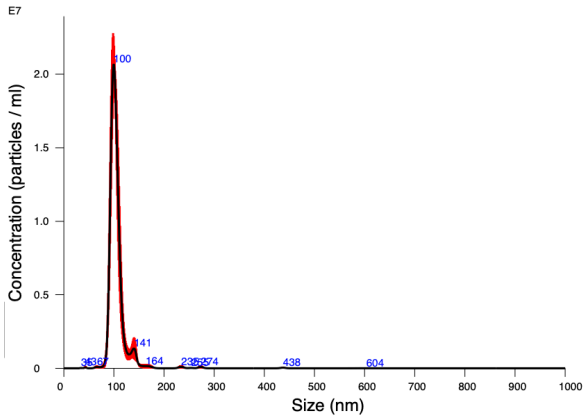

Fig. B.1. Concentration (particles/ml) as a function of size (nm) for control beads (100 nm). beads, used as size control.

B.2 ANOVA tables

Table B.2.1. Ordinary two-way ANOVA table with Sidak and Tukey multiple comparisons tests for EZM.

Ordinary Two-way ANOVA - EZM			
Source of Variation	% of total variation	P value	P value summary
Interaction: Time x genotype	1,707	0,6825	ns
Time	15,52	0,0417	*
Genotype	8,996	0,0519	ns
Tukey's multiple comparisons test			
		Adjusted P Value	Summary
WT			
1.5 months vs. 3 months		0,8467	ns
1.5 months vs. 6 months		0,033	*
3 months vs. 6 months		0,1732	ns
5XFAD			
1.5 months vs. 3 months		0,6712	ns
1.5 months vs. 6 months		0,4076	ns
3 months vs. 6 months		0,8992	ns
Šídák's multiple comparisons test			
		Adjusted P Value	Summary
WT - 5XFAD			
1.5 months		0,471	ns
3 months		0,2945	ns
6 months		0,9475	ns

Table B.2.2. Ordinary two-way ANOVA table with Sidak and Tukey multiple comparisons tests for NTA of size of particles in plasma samples.

Ordinary Two-way ANOVA - Size of particles			
Source of Variation	% of total variation	P value	P value summary
Interaction: Time x genotype	25,87	0,0053	**
Time	55,14	0,0001	***
Genotype	0,3896	0,6536	ns
Tukey's multiple comparisons test			
		Adjusted P Value	Summary
WT			
1.5 months vs. 3 months		ns	0,7708
1.5 months vs. 6 months		ns	0,6203
3 months vs. 6 months		ns	0,2901
5XFAD			
1.5 months vs. 3 months		**	0,002
1.5 months vs. 6 months		ns	0,1249
3 months vs. 6 months		****	<0,0001
Šídák's multiple comparisons test			
		Adjusted P Value	Summary
WT - 5XFAD			
1.5 months		ns	0,8636
3 months		*	0,024
6 months		ns	0,119

Table B.2.3. Ordinary two-way ANOVA table with Sidak and Tukey multiple comparisons tests for NTA of number of particles in plasma samples.

Ordinary Two-way ANOVA - Number of particles			
Source of Variation	% of total variation	P value	P value summary
Interaction: Time x genotype	0,4121	0,9294	ns
Time	43,82	0,0033	**
Genotype	0,3201	0,7392	ns
Tukey's multiple comparisons test			
		Adjusted P Value	Summary
WT			
1.5 months vs. 3 months		ns	0,9729
1.5 months vs. 6 months		*	0,0203
3 months vs. 6 months		ns	0,1846
5XFAD			
1.5 months vs. 3 months		ns	0,9757
1.5 months vs. 6 months		ns	0,0653
3 months vs. 6 months		ns	0,1127
Šídák's multiple comparisons test			
		Adjusted P Value	Summary
WT - 5XFAD			
1.5 months		ns	0,9724
3 months		ns	0,9992
6 months		ns	0,9484

Table B.2.4. Ordinary two-way ANOVA table with Sidak and Tukey multiple comparisons tests for RT-qPCR analysis of Rny3 gene expression in brain tissue.

Ordinary Two-way ANOVA - *Rny3* expression in brain tissue			
Source of Variation	% of total variation	P value	P value summary
Interaction: Time x genotype	16,24	0,0868	ns
Time	13,4	0,1273	ns
Genotype	13,78	0,0426	*
Tukey's multiple comparisons test			
		Adjusted P Value	Summary
WT			
1.5 months vs. 3 months		ns	0,9306
1.5 months vs. 6 months		ns	0,9999
3 months vs. 6 months		ns	0,8968
5XFAD			
1.5 months vs. 3 months		*	0,0384
1.5 months vs. 6 months		*	0,0283
3 months vs. 6 months		ns	0,9352
Šídák's multiple comparisons test			
		Adjusted P Value	Summary
WT - 5XFAD			
1.5 months		*	0,0189
3 months		ns	0,9918
6 months		ns	0,9887